Identification of a new type of PBX1 partner that contains zinc finger motifs and inhibits the binding of HOXA9-PBX1 to DNA.

Audrey Laurent, Réjane Bihan, Stéphane Deschamps, Daniel Guerrier, Valérie Dupé, Francis Omilli, Agnès Burel, Isabelle Pellerin

Mechanisms of Development 124 (2007) 364–376

www.elsevier.com/locate/modo

Identification of a new type of PBX1 partner that contains zinc finger motifs and inhibits the binding of HOXA9-PBX1 to DNA

Audrey Laurent [1], Réjane Bihan [1], Stéphane Deschamps, Daniel Guerrier, Valérie Dupé, Francis Omilli, Agnès Burel, Isabelle Pellerin *

UMR CNRS 6061, Génétique et Développement, IFR 140, Faculté de Médecine, Université de Rennes 1, Campus Villejean, 2 avenue du Professeur Léon Bernard, CS34317, F-35043 Rennes Cedex, France

Received 22 December 2006; received in revised form 30 January 2007; accepted 31 January 2007
Available online 8 February 2007

Abstract

PBX1 belongs to the TALE-class of homeodomain protein and has a wide functional diversity during development. Indeed, PBX1 is required for haematopoiesis as well as for multiple developmental processes such as skeletal patterning and organogenesis. It has furthermore been shown that PBX1 functions as a HOX cofactor during development. More recent data suggest that PBX1 may act even more broadly by modulating the activity of non-homeodomain transcription factors. To better understand molecular mechanisms triggered by PBX1 during female genital tract development, we searched for additional PBX1 partners that might be involved in this process. Using a two hybrid screen, we identified a new PBX1 interacting protein containing several zinc finger motifs that we called ZFPIP for Zinc Finger PBX1 Interacting Protein. We demonstrated that ZFPIP is expressed in embryonic female genital tract but also in other PBX1 expression domains such as the developing head and the limb buds. We further showed that ZFPIP is able to bind physically and *in vivo* to PBX1 and moreover, that it prevents the binding of HOXA9/PBX complexes to their consensus DNA site. We suggest that ZFPIP is a new type of PBX1 partner that could participate in PBX1 function during several developmental pathways.

Keywords: PBX1; HOX; Cofactor; Genital tract

1. Introduction

PBX1 (pre-B-cell leukemia transcription factor 1) was initially isolated as a proto-oncogene in human leukaemia induced by the expression of the oncogenic fusion E2a-PBX1 protein (Kamps et al., 1990; Nourse et al., 1990). PBX1 belongs to the PBC group of the TALE class of homeodomain proteins that comprises PBX1, PBX2, PBX3 (Monica et al., 1991), PBX4 (Wagner et al., 2001), zebrafish Lazarus or lzr (Popperl et al., 2000; Waskiewicz et al., 2001), Drosophila Extradenticle or Exd and Caenorhabditis elegans Ceh-20 (Shanmugam et al., 1999; Shen et al., 1999). Several studies have demonstrated that PBC proteins were able to interact with a subset of HOX proteins and as such been considered as essential HOX cofactors involved in developmental gene regulation (reviewed in (Moens and Selleri, 2006).

Inactivation of *PBC* genes in different models have demonstrated that PBC proteins make critical contributions to cell fate and segmental patterning during development (reviewed in Moens and Selleri, 2006). In particular, loss-of-function studies have demonstrated a critical role for PBX1 in cellular proliferation and patterning and suggest its involvement in numerous regulatory pathways (Selleri et al., 2001). Indeed, *PBX1* mutants die at embryonic day 15/16 with severe hypoplasia or aplasia of multiple organs and widespread patterning defects of the axial and appendicular skeleton. Amongst abnormal organogenesis

* Corresponding author. Tel.: +33 2 23 23 44 63; fax: +33 2 23 23 44 78.
E-mail address: isabelle.pellerin@univ-rennes1.fr (I. Pellerin).
[1] Both authors have equally contributed to the work.

0925-4773/$ - see front matter © 2007 Elsevier Ireland Ltd. All rights reserved.
doi:10.1016/j.mod.2007.01.008

processes observed in these mutants, the urogenital system is severely affected with a markedly reduced urogenital ridge outgrowth and impaired differentiation of the mesonephros and kidneys. In addition, the Müllerian ducts which represent the antecedent of the female genital tract (i.e. oviducts, uteri and vagina) and are normally formed in E12.0 wild-type embryos, are lacking in both male and female mutants while the anlagen of the male genital tract, the Wölffian ducts are present (Schnabel et al., 2001).

Although some of the *PBX1* mutant phenotypes are similar to *HOX* mutants and can be thus attributed to effects on HOX function, some other aspects of the *PBX1*$^{-/-}$ mouse suggest that PBX1 may act more broadly in non HOX expressing embryonic area and/or in HOX independent pathways. In particular, the implication of *HOX* genes during female genital tract development differs quite significantly from that of *PBX1*. The Müllerian ducts do not form in *PBX1* mutant animals (Schnabel et al., 2003) whereas inactivation of the *HOXA10*, *HOXA11*, *HOXA13* or *HOXD13* gene provokes morphological defects along the proximodistal axis of the female reproductive tract that could initially differentiate (reviewed in Taylor, 2000). The absence of Müllerian ducts in *PBX1* mutants indicates the early involvement of the gene in this organogenesis. In addition, the gene seems to be required throughout female genital tract development as suggested by its constant expression during this process (Schnabel et al., 2001) and until puberty (Dintilhac et al., 2005).

In the aim to better understand the molecular mechanisms triggered by PBX1 during female genital tract development, we searched for new partners that might be involved in higher-order molecular gene regulation complexes during this organogenesis. For this purpose, we performed a two hybrid screen using full length PBX1B as bait and a cDNA library constructed with RNAs extracted from differentiating Müllerian ducts of E16.5 to E18.5 embryos.

By this way, we identified a new PBX1 interacting protein containing several zinc finger motifs that we called ZFPIP for Zinc Finger PBX1 Interacting Protein. We demonstrated that ZFPIP is expressed in embryonic female genital tract but also in other PBX1 expression domains such as the developing head and the limb buds. We further showed that ZFPIP is able to bind physically and *in vivo* with PBX1 and moreover, that it prevents the binding of HOXA9/PBX complexes to their consensus DNA site. We therefore suggest that ZFPIP is a new type of PBX1 partner that could participate in PBX1 function during several developmental pathways.

2. Results

2.1. Identification of a novel PBX1B partner expressed during female genital tract development

To isolate cDNAs encoding proteins that associate with PBX1B during female genital tract development, we first created a randomly primed cDNA library from polyA + RNAs from Müllerian ducts and used full-length PBX1B as bait. Prior to library screening, we verified that PBX1B possessed no intrinsic transcriptional activation of the reporter genes (not shown). Out of 1.2×10^5 transformants screened, 50 positive clones were finally selected for sequencing analysis based on two nutritional markers as well as by *lacZ* and *MEL1* reporter expression. Amongst these 50 clones, only 20 cDNAs were in frame with the Gal4 ORF in the prey plasmids. Two of these clones were identified as independent, overlapping *PBX1* cDNAs. Since it has been demonstrated, using different approaches, that PBX1 can homodimerize (Calvo et al., 1999), the presence of these clones validated the screen.

One of the positive clones was further studied. Fig. 1A shows that the corresponding peptide is able to activate reporter genes in the two hybrid system whereas no such

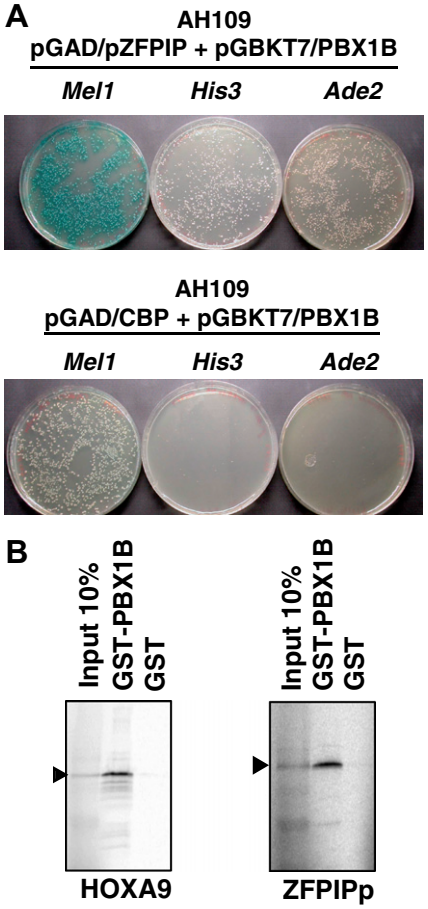

Fig. 1. Identification of a new putative PBX1 partner. (A) Positive clones identified by the two hybrid screen were isolated and tested by a secondary screen. Using the full length PBX1B protein as bait, one selected clone corresponding peptide was able to activate reporter genes (*Mel1*, *His3*, *Ade2*) in the two hybrid system whereas no such activation was obtained with CBP as a control protein. (B) This clone was further analyzed by GST-pull down. Radio-labelled *in vitro* translated putative partner was incubated with Glutathione–Sepharose beads loaded with either GST or GST-PBX1B. After several washes, proteins were eluted and analyzed on SDS–PAGE. Compared by GST pull down, the binding of the selected clone encoding peptide with PBX1B was similar to the binding of HOXA9.

activation is obtained with CBP (CREB Binding Protein) as a control protein. We thus used GST pull-down to compare the interaction between this peptide and PBX1B with the binding of PBX1B and its well characterized partner i.e. HOXA9. Indeed, while most HOX proteins bind to PBX1 in the presence of DNA, HOXA9 can heterodimerize to PBX1 without DNA (Shen et al., 1999; Dintilhac et al., 2005). As shown in Fig. 1B, the selected peptide exhibited a binding for PBX1B that was similar to that of HOXA9.

2.2. The novel PBX1B partner corresponds to a large zinc finger protein that is nuclear targeted

Sequencing of selected clone showed that it contained a 650 bp cDNA. In order to reconstitute the full-length cDNA, we searched for mouse ESTs in several libraries and used the available cDNA sequence of the human homologous *ZFPIP* cDNA (Accession No.: NP 067047). This *in silico* analysis revealed that the partial cDNA that we isolated was encompassed in a full-length 8 kb cDNA that encodes a 250 kDa protein of unknown function but that contains 34 classical Cys2His2 (C2H2) zinc finger motifs spread throughout the molecule. Three of these zinc finger motifs located at the C-terminal end of the protein form a putative DNA binding domain that is similar but not identical to the one of mammalian Sp-XKLF (Krüppel Like Factors) family members (Fig. 2A). Given the high number of C2H2 motifs found within the protein, we consequently termed it ZFPIP for Zinc Finger PBX1 Interacting Protein. Using the BLAST program, we analysed the peptidic region encoded by the cDNA initially isolated from the screen (this region of the protein was named ZFPIPp for partial ZFPIP). We showed that within this PBX1B interacting region, two domains of 33 and 44 amino acids were highly conserved from tetraodon to human (Fig. 2A and B) suggesting an important role of this particular region. The analysis of this conserved region showed the presence of a Nuclear Localization Signal (NLS) that might be involved in nuclear targeting of the protein. Indeed, only the N-ZFPIP and ZFPIPp proteins were addressed to the nucleus whereas the C-ZFPIP protein which does not contain the NLS was not found in the nucleus of the cells (Fig. 2C).

2.3. ZFPIPp associates in vitro and vivo with PBX1

The interaction between ZFPIP and PBX1B observed in the two hybrid system and by GST pull down was further analyzed. We first confirmed the *in vitro* interaction of both partners using GST-ZFPIPp and *in vitro* translated PBX1B protein. As shown on Fig. 3A, PBX1B associated with GST-ZFPIPp but not with GST alone. Similar experiments were performed with PBX1A and demonstrated an equivalent binding between ZFPIPp and PBX1A, showing that ZFPIP could be a new partner of both PBX1 isoforms (not shown). Moreover, *in vivo* interaction between PBX1B and ZFPIP in mammalian cells was corroborated by co-immunoprecipitation of FLAG-ZFPIPp and HA-PBX1B expressed in Cos-7 cells. Indeed, PBX1B and ZFPIPp were co-immunoprecipitated (Fig. 3B, lanes 3 and 6) with anti-FLAG M2 beads as efficiently as the PBX1B/HOXA9 heterodimer (Fig. 3B, lanes 1 and 4) whereas no PBX1B was immunoprecipitated when co-expressed with eRF1 (eukaryotic peptide chain Release Factor 1) used as a negative control protein (Fig. 3B, lane 5). We thus mapped the ZFPIP interaction domain as residues 215–241 in PBX1B (Fig. 3C) and showed that it contained the most N-terminal located NLS motif of the protein (NLS1, Fig. 3D).

2.4. PBX1 and ZFPIP are both present in embryonic female genital tract protein extracts

Expression pattern of PBX1 and its involvement during urogenital morphogenesis have been well described (Schnabel et al., 2001, 2003). We recently showed that PBX1B was expressed throughout genital tract development until the onset of puberty (Dintilhac et al., 2005). Since the library used in the two hybrid screening was performed with cDNAs obtained from female genital tracts of E16.5 to E18.5 embryos, the presence of *PBX1B* and *ZFPIP* transcripts in this organ was expected. Using three sets of primers complementary to sequences located throughout the cDNA (Fig. 4A), we confirmed by RT PCR the presence of *ZFPIP* transcripts in the embryonic genital tract (Fig. 4A, lane 1, 2, 3) as well as the presence of both transcripts of the *PBX1* gene (*PBX1A* and *PBX1B*). However, although *ZFPIP* and *PBX1* gene transcription was evidenced by RT-PCR, the presence of the corresponding ZFPIP protein in this embryonic organ could be questioned. To address this point, we produced an antibody raised against ZFPIP (Fig. 2A). The specificity of the antibody was tested in immunocytochemistry and Western blot experiments. Fig. 4B corresponds to FLAG-ZFPIPp expressing Cos-7 cells that were immunocytochemically stained with ZFPIP antibodies or depleted antibodies (see Section 4). As shown, a nuclear immunostaining was clearly observed in FLAG-ZFPIPp expressing cells incubated with α-ZFPIP antibodies whereas no signal was detected in cells incubated with depleted serum. The same nuclear staining was observed when FLAG-ZFPIPp expressing cells were analysed with α-FLAG antibodies (data not shown). Protein extracts from FLAG-ZFPIPp expressing Cos-7 cells were analyzed by western blotting using the same antibodies. An immunoreactive band was only observed on the membrane incubated with α-FLAG or α-ZFPIP antibodies whereas no band was observed with depleted antibodies (Fig. 4C). Given the specificity of the ZFPIP antibody, we thus used it to detect the endogenous protein in embryonic genital tract extracts. Since the antibody was targeting in a highly conserved region of the protein (Fig. 2), we used protein extracts from female embryonic bovine genital tracts to overcome the difficulty of getting sufficient proteins from an embryonic organ in mouse. As shown on Fig. 4D, an immunoreactive band

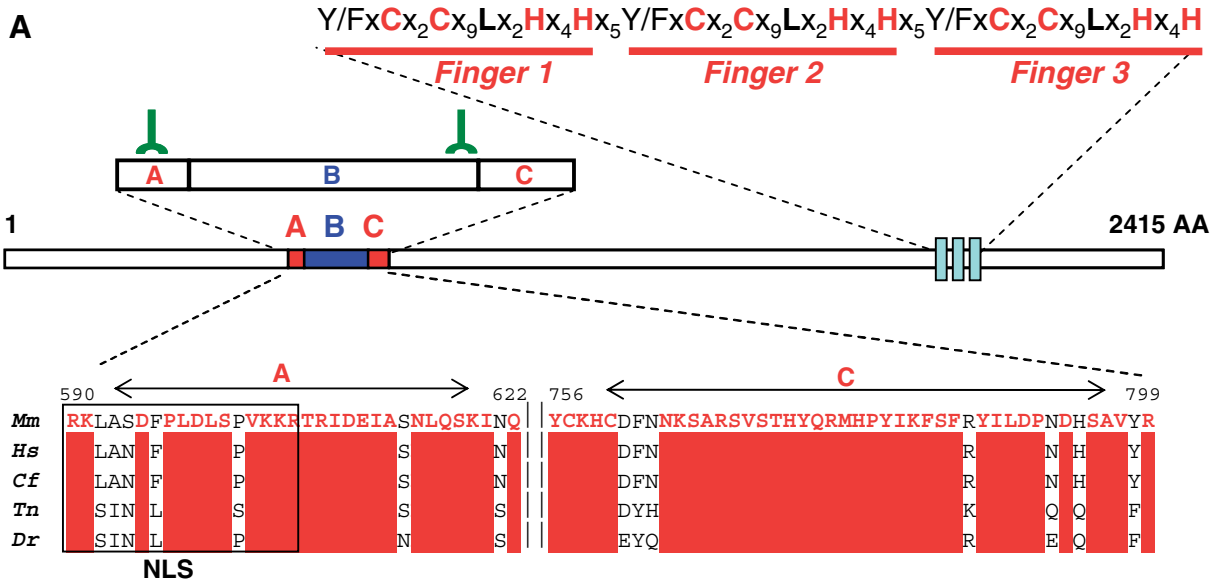

B

% identity within ZFPIP						
	A *590-622*	B *623-755*	C *756-799*	NLS	A+B+C (ZFPIPp)	ZFPIP (full length)
Homo	97 %	83 %	100 %	94 %	89 %	90 %
Canis	97 %	83 %	100 %	94 %	89 %	83 %
Tetraodon	82 %	47 %	86 %	71 %	44 %	51 %
Danio	82 %	28 %	86 %	77 %	47 %	44 %

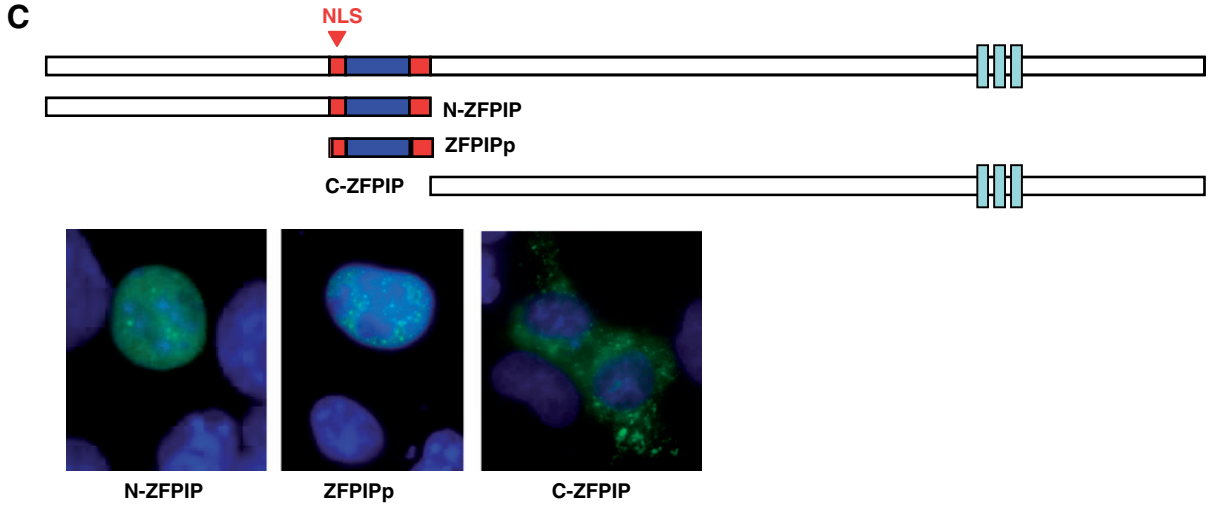

Fig. 2. *ZFPIP* cDNA encodes a new type of C2H2 zinc finger protein. (A) Sequence analysis of the selected clone indicates that it belongs to a full-length 8 kb cDNA that encodes an uncharacterized protein containing a NLS (Nuclear Targeted Sequence indicated in the rectangle) and a putative DNA binding domain with three zinc fingers. Two antibodies were generated against two peptides of the protein and are indicated in green in (A). (B) Within the putative ZFPIP protein, the region corresponding to the peptide isolated from the two hybrid screen contains two highly conserved domains (domains A and C) and a bipartite NLS. (C) Immunocytochemistry were performed on Cos-7 cells transiently transfected with FLAG-N-ZFPIP, FLAG-ZFPIPp and FLAG-C-ZFPIP proteins using FLAG antibodies (α-FLAG). Specific staining was detected with a fluorescein isothiocyanate conjugated secondary antibody and nuclear staining by DAPI. Only the FLAG-N-ZFPIP and FLAG-ZFPIPp proteins that contain the NLS were targeted to the nucleus of Cos-7 cells whereas the FLAG-C-ZFPIP proteins remained in the cytoplasm.

corresponding to a protein of approximately 250 kDa was specifically observed in embryonic genital tract extracts when the blot was analyzed with the ZFPIP antibody but absent in embryonic liver and Cos-7 cells. No signal was observed when using the depleted serum (data not shown).

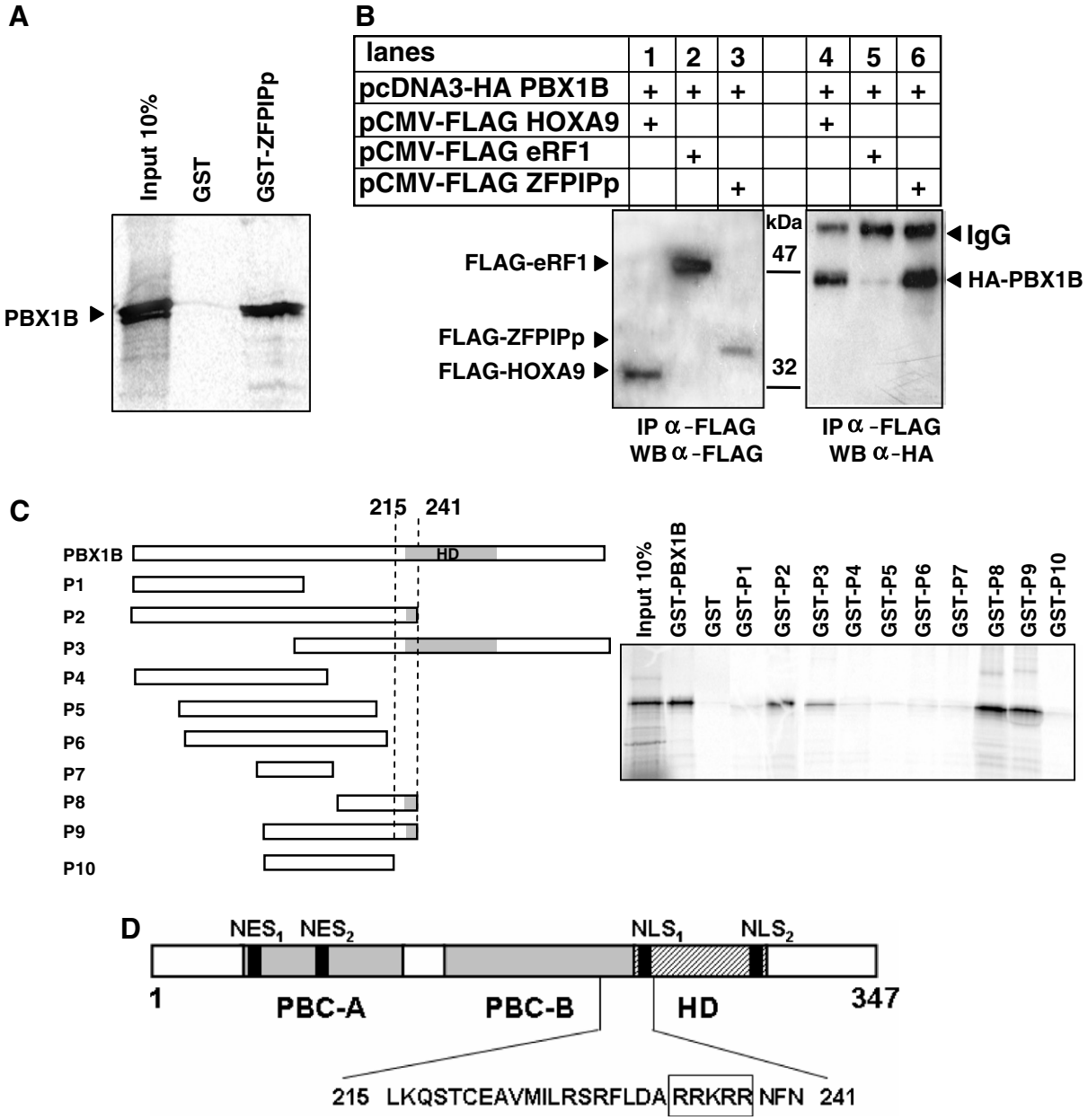

Fig. 3. ZFPIP physically binds recombinant GST-PBX1B and co-precipitates with PBX1B in protein Cos-7 cells extracts. (A) Radiolabelled *in vitro* translated PBX1B was incubated with Glutathione–Sepharose beads loaded with either GST or GST-ZFPIPp. After several washes, proteins were eluted and analyzed on SDS–PAGE. (B) Protein extracts containing HA-PBX1B in combination with FLAG-HOXA9 (lane 1, 4) or FLAG-eRF1 (lane 2, 5) or FLAG-ZFPIPp (lane 3, 6) were incubated with agarose anti-flag M2 beads as described in methods. Proteins bound on the beads were eluted with a 0.1 M glycine solution and analyzed on SDS–PAGE. Western blots were realized with anti FLAG antibodies (α-FLAG) and anti HA antibodies (α-HA). (C) Mapping of the ZFPIP interaction domain in PBX1B. Different truncated PBX1B proteins were expressed as GST fusion proteins and incubated with ^{35}S-ZFPIPp protein. GST pull down were performed as described in methods and demonstrated that the interaction domain of PBX1B with ZFPIP corresponded to amino-acids 215–241. (D) The ZFPIP interaction domain (AA 215–241) contains one of the NLS identified for PBX1 (NLS1). The two domains conserved among PBC family proteins, PBC-A and PBC-B, as well as the HD, NLS and NES are indicated.

2.5. ZFPIP and PBX1 share similar timing and overlapping pattern of expression during embryogenesis

In this work, we identified a novel zing finger protein that interacts physically with PBX1B and that is co-expressed within the developing genital tract. In order to investigate whether ZFPIP could be a more general PBX1 partner involved in other aspects of mouse development, we further studied its overall expression during embryogenesis. Using whole mount *in situ* hybridization, we observed that *ZFPIP* mRNA was mostly located in the head and limb buds of E9.5 and E11.5 embryos (Fig. 5A). In the developing head at E9.5 and E10.5, *ZFPIP* expression was intense in the forebrain (FB), the midbrain (MB) as well as in the first and second branchial arches (BA). In particular, in the first pharyngeal arch,

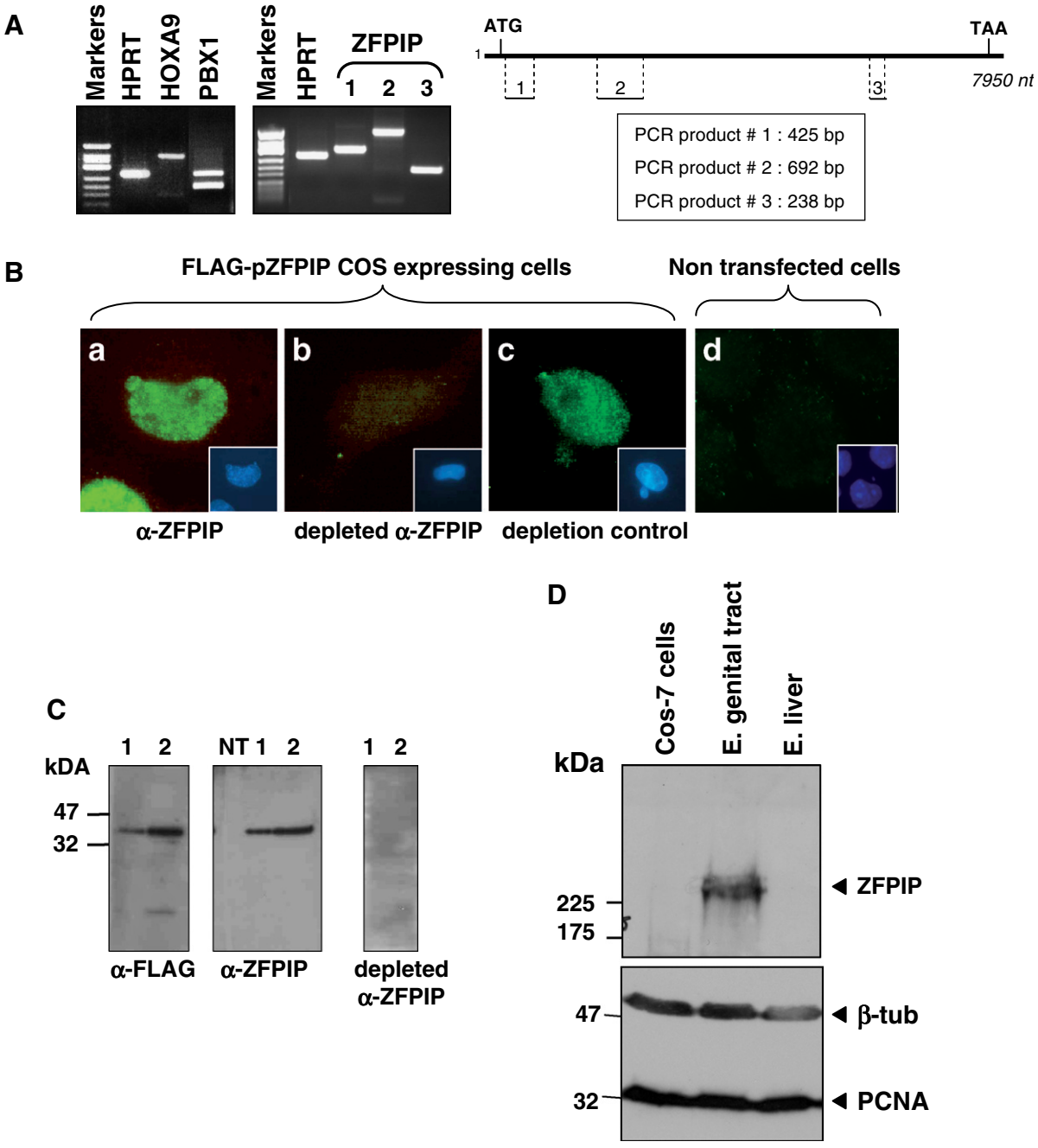

Fig. 4. ZFPIP is expressed in embryonic female genital tract. (A) RT-PCR was performed with RNAs extracted from embryonic female genital tracts using specific primers of *HPRT*, *HOXA9*, *PBX1* and 3 different sets of primers complementary to *ZFPIP* (see Table 1). PCR products were analyzed and visualized by an ethidium bromide-stained 2% agarose gel along with molecular markers (Markers) corresponding to ΦX 174/HinfI (Promega). (B) Immunocytochemistry was performed with anti ZFPIP antibody (α-ZFPIP) and a fluorescein conjugated secondary antibody (a). Controls were performed with an antibody depleted by absorption with an excess of recombinant GST-ZFPIP (b, depleted α-ZFPIP) or with an excess of GST (c, depletion control) before secondary antibody addition. An immunocytochemistry experiment was also performed on non-transfected cells (d). Fluorescence was detected under UV light using a Leica microscope with a final magnification of 500×. The staining of nuclei with DAPI (blue) is shown in small square boxes. (C) Protein extracts prepared from cells expressing FLAG-ZFPIPp (lane 1, 2) or not expressing FLAG-ZFPIPp (NT) were loaded on SDS–PAGE and analyzed by western blots using α-FLAG, α-ZFPIP and depleted α-ZFPIP antibodies. Protein markers (in kDa) are indicated on the left of the blot. (D) Proteins were prepared from embryonic tissues (female genital tract and liver) or from Cos-7 cells and then were separated on SDS–PAGE. Proteins were transferred onto PVDF membranes and incubated with α-ZFPIP, β-tubulin or PCNA antibodies. A specific band is visualized in genital tract extracts and the migration of the corresponding proteins allowed us to correlate this immunoreactive band to the ZFPIP protein. Markers (in kDa) are indicated on the left of the blot.

expression was distinctively detected in the maxilla (Mx) and mandibular (Md) prominences. In E11.5 embryos (Fig. 5A) and E12.5 (data not shown), ZFPIP expression was still observed in developing limbs and in the cerebral hemisphere of the head. In addition to these experiments, we performed real time reverse transcription PCR from

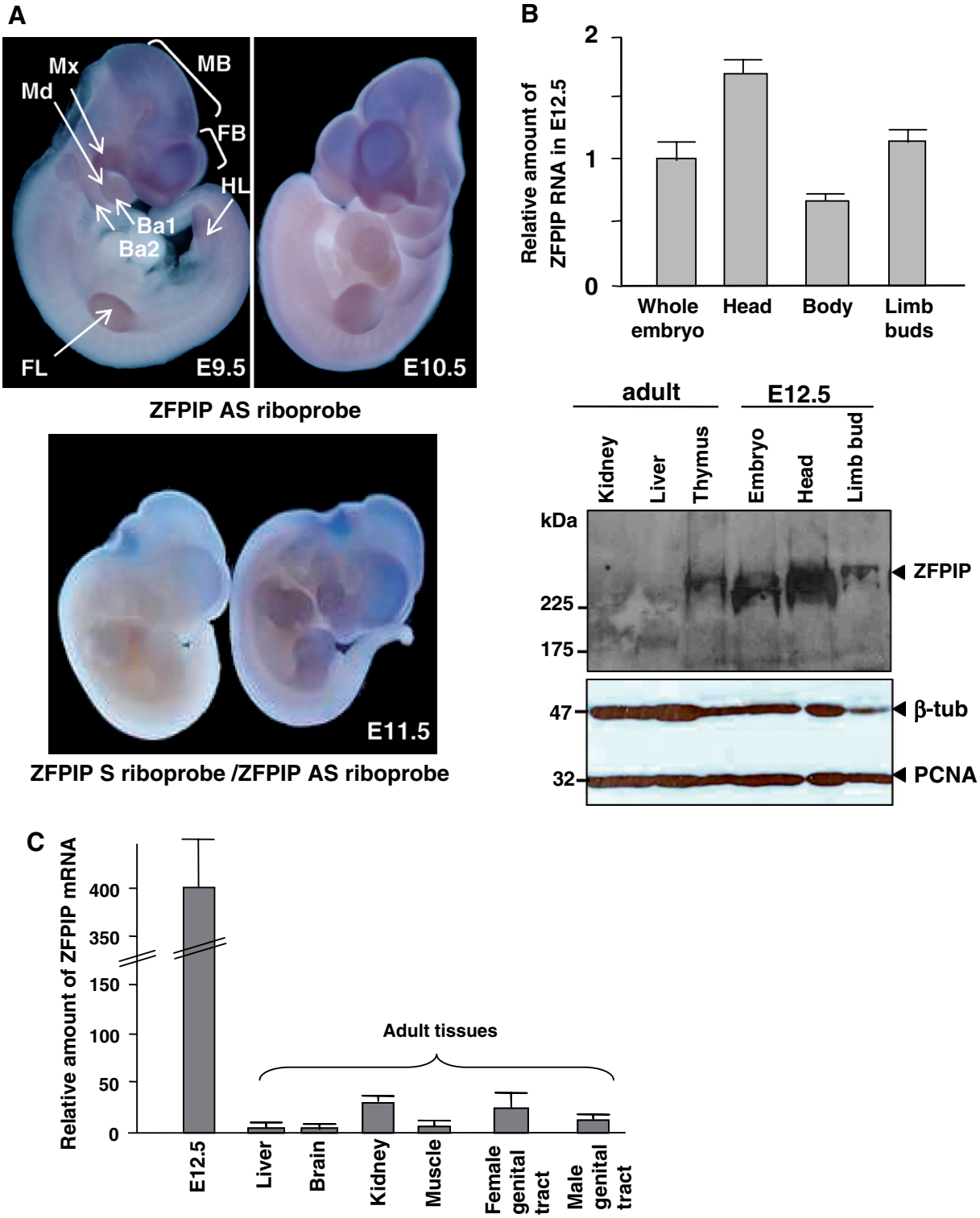

Fig. 5. ZFPIP is highly expressed in developing head and limb buds. (A) Whole-mount *in situ* hybridization using digoxigenin-labelled *ZFPIP* riboprobes were performed on E9.5; E10.5 and E11.5 embryos. An intense staining is observed in the forebrain (FB), the midbrain (MB) as well as in the first and second branchial arches (Ba1, Ba2) on E9.5 and E10.5 embryos. Arrows indicate *ZFPIP* expression in the first pharyngeal arch at the level of the maxilla (Mx) and mandibular (Md) prominences, in the forelimb (FL) and the hindlimb (HL). Two E11.5 embryos hybridized with either a *ZFPIP* sens riboprobe (ZFPIP S, on the left) or a *ZFPIP* antisens riboprobe (ZFPIP AS, on the right) are shown and illustrate a specific *ZFPIP* expression in developing limbs and in the cerebral hemisphere. (B) *ZFPIP* transcript and its product are more abundant in the developing head. Real-time reverse transcriptase-PCR experiments were performed with RNAs extracted from parts of E12.5 embryos (whole embryo, head, body, limb buds) and specific *ZFPIP* primers (see Table 1) as described in methods. Western blots were prepared from embryos and different parts of mouse embryos (whole embryos, head and limb buds of E12.5) as well as in adult mouse tissues (kidney, liver, thymus) and performed using either α-ZFPIP, β-tubulin or PCNA antibodies. Protein markers (in kDa) are indicated on the left of the blot. (C) *ZFPIP* is highly expressed during embryogenesis compared to adult organs. Relative expression of *ZFPIP* was calculated using HPRT as internal control. Experiments were run at least three times from different RNA extractions.

RNAs extracted from either whole or parts of E12.5 embryos (head, limb buds and body). As shown in Fig. 5B, the level of *ZFPIP* mRNAs was higher in the head and the limb buds compared to the level of the transcripts in the rest of the embryo (body). Protein extracts were also prepared from different adult tissues and embryonic regions to be analyzed by Western blot. Using ZFPIP antibodies described above, we detected an intense immunoreactive band corresponding to the ZFPIP protein in embryonic extracts from the head whereas lower signal was obtained in extracts prepared from whole embryos and limb buds. Although no protein was detected in adult liver and kidney, an immunoreactive band was observed in adult thymus. In addition, we analyzed the level of *ZFPIP* mRNA during embryogenesis and in several adult tissues. As demonstrated on Fig. 5C, the level of *ZFPIP* in E12.5 embryo was much higher (10- to 40-fold) than in any other adult organ tested (liver, brain, kidney, muscle, female and male genital tract).

Since ZFPIP expression was mostly detected in the forebrain and the midbrain, we performed *in situ* hybridization on frontal sections of E11.5 embryos. As shown in Fig. 6A, ZFPIP was expressed throughout the wall of the telencephalic vesicle. In E11.5 embryos, ZFPIP was expressed at high level in area that expressed PBX1 i.e. the medial and lateral ganglionic eminence (respectively, MGE and LGE) (Toresson et al., 2000).

We finally compared, by real time reverse transcription PCR, the time course of *ZFPIP* expression to that of *PBX1* during embryogenesis. As shown in Fig. 6B we observed that both genes shared similar kinetics of expression with a peak at mid-gestation (E10.5) and a decrease at E15.5 until birth (data not shown).

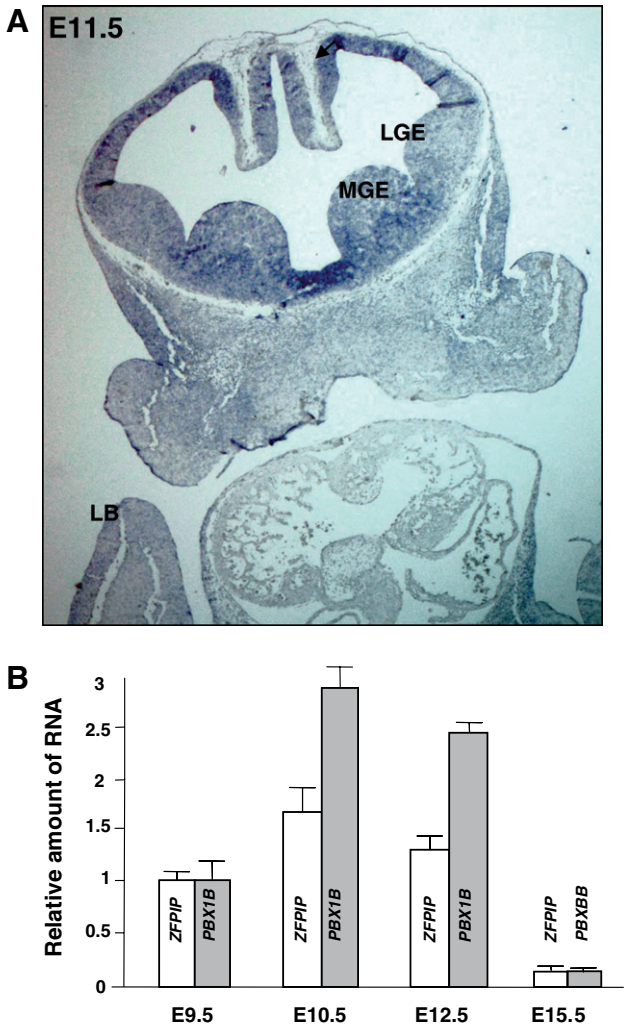

Fig. 6. *ZFPIP* shares similar pattern and kinetic of expression than PBX1. (A) Frontal sections of E11.5 embryos were performed using *ZFPIP* AS or *ZFPIP* S riboprobes. ZFPIP mRNA was detected throughout the wall of the telencephalon and E11.5 embryo and in limb buds. These expression domains correspond to area where PBX1 was shown to be also expressed (Toresson et al., 2000). (B) Real-time reverse transcriptase PCR experiments demonstrate that *ZFPIP* and *PBX1* share similar kinetic of expression with a peak at 10.5 days post-coïtum (pc) and a decrease at 15.5 days pc.

2.6. ZFPIP abrogates cooperative PBX1-HOXA9 binding to their consensus site

The most well-known biological property of PBC proteins consists of forming complexes with HOX proteins and consequently increasing their binding specificity on specific DNA motifs. Thus, in order to gain insights into the functional role of ZFPIP on PBX1, we investigated whether this new partner could affect the binding of HOXA9/PBX to DNA. We chose as a partner, HOXA9 which is known to form a stable heterodimer with PBX1 (LaRonde-LeBlanc and Wolberger, 2003). EMSA were performed using a procedure suitable to the binding of HOXA9/PBX1 on its consensus DNA site, as previously reported by (Shen et al., 1997a). In these experimental conditions, *in vitro* translated HOXA9 and/or PBX1 proteins (PBX1A and PBX1B) were incubated with a HOXA9/PBX consensus DNA site and protein extracts from bacteria expressing either GST-ZFPIPp or GST. From the EMSA shown in Fig. 7, we observed that radiolabelled HOXA9/PBX consensus DNA site was shifted by *in vitro* translated HOXA9, HOXA9/PBX1A and HOXA9/PBX1B. As previously demonstrated (Asahara et al., 1999; Shen et al., 1997b), the full length PBX1 protein was not able to bind DNA (data not shown). Interestingly, the addition of GST-ZFPIPp poorly affected the DNA interaction of HOXA9 as a monomer while it reduced considerably the association of DNA/HOXA9/PBX1A and DNA/HOXA9/PBX1B. In contrast, the addition of GST did not influence HOXA9/PBX1 DNA binding.

3. Discussion

Using a yeast genetic two-hybrid screen with the full length PBX1B as bait, we isolated from an embryonic female genital tract library, a partial cDNA that corresponded to a new type of large zinc finger protein. The interaction between PBX1 and this new zinc finger protein

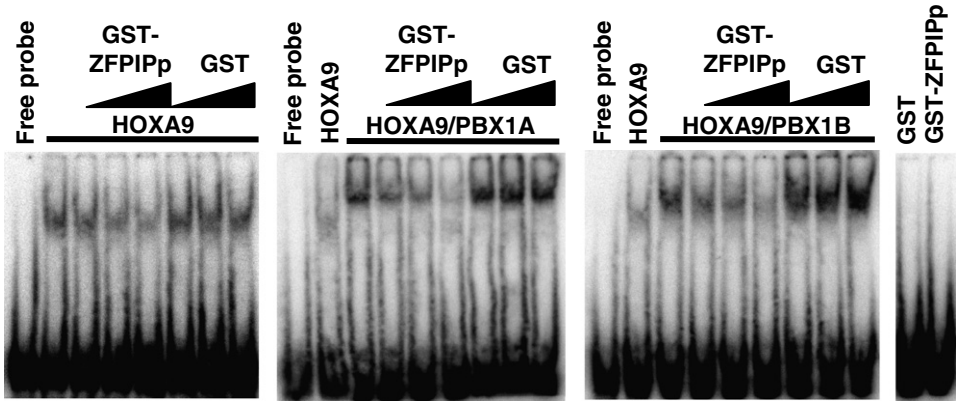

Fig. 7. ZFPIP prevents the binding of the HOXA9/PBX complex on its consensus DNA site. EMSA experiments were performed using *in vitro* translated HOXA9, PBX1A, PBX1B proteins and an oligonucleotide containing HOXA9/PBX consensus DNA site as previously described (Shen et al., 1997a). Bacteria lysates expressing GST or GST-ZFPIPp were added to binding reactions containing either HOXA9 or HOXA9 plus PBX1 proteins. Essentially identical results were obtained when GST-ZFPIPp was added to the trimmers HOXA9/PBX1B/DNA or HOXA9/PBX1A/DNA, demonstrating an inhibition of both complexes by ZFPIPp.

was further validated *in vitro* by pull-down experiments and *in vivo* by co-precipitation of both partners transiently expressed in mammalian cells. This new protein has been consequently designated by ZFPIP for Zing Finger PBX1 Interacting Protein. The study of *ZFPIP* gene expression revealed that *ZFPIP* and *PBX1* shared similar spatial and temporal pattern of expression. Moreover, the peptidic region involved in the interaction between PBX1 and ZFPIP was shown to inhibit HOXA9/PBX binding to DNA. These overall experiments let us to hypothesize that ZFPIP is a new PBX1 partner that participates with PBX1 to female genital tract development and might also be more broadly involved in gene regulation complexes during embryogenesis.

3.1. ZFPIP might take part of a transcription regulation complex that contains HOX and PBX proteins

Members of PBC gene family were initially identified as genes involved in embryogenesis and as protooncogenes in various forms of leukemia. Subsequent biochemical and genetic studies revealed that PBC proteins act as cofactors of HOX proteins. HOX proteins are homeodomain transcription factors that regulate cell fate decisions in many tissues during early embryonic development and subsequent organogenesis. PBC proteins cooperate with HOX to enhance their function by improving their affinity and specificity for specific promoter elements (reviewed in Mann and Affolter, 1998). In order to better understand the molecular mechanisms triggered by PBX1, we searched for additional cofactors and identified a new partner that belongs to the zinc finger super family protein and that we called ZFPIP.

In silico analysis of the ZFPIP protein led us to identify 34 classical C2H2 zinc finger DNA binding modules which structure were first reported in 1989 (Lee et al., 1989) and were then found in many transcription factors. Furthermore, three of these zinc finger modules constitute a triplet at the C-terminus end of the protein that is close but not identical to the DNA binding domain found in Krüppel like factors. The presence of this zinc finger triplet that constitutes a likely functional DNA binding domain within a protein that contains 31 other C2H2 zinc finger DNA binding module, suggests a strong ability of ZFPIP to bind DNA. However, the fact that no other putative functional domain, such as repression or activation domains, has been identified within the protein, questioned the role of ZFPIP as a transcription factor. Our EMSA data showed that the HOXA9/PBX1/DNA complex is inhibited by ZFPIPp. In addition, no HOXA9/DNA complex is restored under these conditions suggesting that ZFPIPp does not compete with HOXA9 for binding to PBX. Indeed, when ZFPIPp is added to the HOXA9/PBX1/DNA complex, HOXA9 protein is not released and able to bind DNA as a monomer. These results might be explained by the formation of a trimeric HOXA9/PBX1/ZFPIP complex that is not able to bind the HOXA9/PBX1 DNA consensus site. One can hypothesize that ZFPIP could keep HOXA9/PBX1 away from their DNA binding sites and direct the proteins to other regulatory sites. However, given the fact that EMSA experiments were performed with a partial part of the ZFPIP protein, the behaviour of the full length protein within a regulatory complex including PBX1 and HOX *in vivo* may be different. Further biochemical characterization of the full length protein and its role on HOX/PBX DNA binding will be necessary to better understand its mode of action.

3.2. PBX1 might constitute a physical link between HOX and zinc finger proteins

Several studies from *Drosophila* have highlighted the fact that zinc finger transcription factors establish specific fields of expression throughout embryo and are required for the specification of segment identity (review in Mahaffey, 2005). In a genetic screen for potential HOX cofactors,

C2H2 zinc finger encoding genes, *disconnected* (*disco*), *disconnected-related* (*disco-r*) and *buttonhead* (*btd*) were shown to be involved in *Drosophila* head development (Mahaffey et al., 2001; Schock et al., 2000) while *t-shirt* (*tsh*) was isolated for its implication in thoracic segments (de Zulueta et al., 1994). Embryos lacking *disco* and *disco-r* genes exhibit head defects similar to those found in embryos lacking the two gnathal *HOX* genes, *Deformed* (*Dfd*) and *Sex comb reduced* (*Scr*) while in the absence of *btd*, mouthpart structures arising from the anterior head segments are missing (Wimmer et al., 1993) (Schock et al., 2000). In addition, the loss of function of *disco* and *disco-r* negatively affects expression of known *Dfd* and *Scr* target genes (Robertson et al., 2004). It has been suggested that HOX proteins can initiate proper cell identity in *Drosophila* only when co-localized with the correct zinc finger partner (Mahaffey, 2005). Homologs of these Drosophila zinc finger proteins have been searched in vertebrates and the expression pattern studies reported so far revealed that they are present in specific HOX overlapping area. Furthermore, the lack of Sp8, which is the *btd* mouse homolog, causes deformities in the head and in other regions of Sp8 expression (Bell et al., 2003) (Kawakami et al., 2004). In addition, the zinc finger containing protein KROX-20 has been shown to synergize in a dosage-dependent manner with HOXA1 to specify the rhombomere 3 identity during hindbrain development (Helmbacher et al., 1998). These studies of zinc finger expression pattern as well as data from their loss of function in mouse suggest that zinc finger proteins collaborate with HOX protein to specify positional identity in mouse. However, no convincing direct link between these zinc finger and HOX proteins were found in vertebrates. The identification of a zinc finger protein that interacts with PBX1 raised the possibility that this protein also interacts with HOX proteins. If this is the case, PBX1 would be the key partner between certain zinc finger and HOX proteins in the process of determining positional identity during development. Such interaction studies are under investigation in our laboratory.

3.3. ZFPIP, a new type of PBX1 partner

PBX1 proteins form complexes with non-HOX homeodomain containing transcription factors like Pdx1 (Goudet et al., 1999), as well as with bHLH proteins like MyoD (Berkes et al., 2004), suggesting that they serve a broader role as transcription cofactors. Recently, it has been suggested that PBX1 may act as "pioneer" transcription factor that penetrate repressive chromatin and mark specific genes for activation by other transcription factors such as HOX or MyoD (Sagerstrom, 2004). In the present work, we present preliminary studies of *ZFPIP* expression pattern showing that the gene is expressed in embryonic areas that contain PBX1 and HOX proteins (embryonic genital tract, limb buds and branchial arches). Consequently interaction between these three partners might be of physiological relevance. In contrast, the forebrain, midbrain and the neural crest cells arising from these encephalic vesicles fail to express any *HOX* gene (Couly et al., 1996; Hunt et al., 1991) but contain members of the PBX families such as PBX1 (Manley et al., 2004; Redmond et al., 1996; Schnabel et al., 2001; Toresson et al., 2000) and PBX3 (Di Giacomo et al., 2006). Our *in situ* analysis revealed that the localization of *ZFPIP* in the telencephalon matched up completely with the expression pattern described for PBX1. Indeed, both genes are expressed in the telencephalic wall, especially in cells of the MGE and LGE (Toresson et al., 2000). In such embryonic area, interaction between ZFPIP and PBX1 proteins is thus conceivable and might be part of an "HOX independent" mode of action of PBX1.

The PBX1 protein has substantial functional diversity during development. Identification of new partners is a key step to understand its molecular mechanisms. ZFPIP is a new type of PBX1 interacting protein that might play a role in "HOX dependent" and "HOX independent" pathways of gene regulation. Future work will aim to understand the role and the molecular mechanisms triggered by this protein.

4. Experimental procedures

4.1. Plasmid constructs

Full-length human PBX1B cDNA was amplified by PCR using SpKBID (kindly provided by M. Cleary, Stanford University) as a template and inserted into *Eco*RI and *Bam*HI sites of the yeast pGBKT7 vector (Clontech). PBX1B cDNA was also cloned into pGEX-6p-1 (Amersham Pharmacia Biotech) to produce bacterially expressed GST tagged proteins as well as into the pcDNA3-HA (gift from J.P. Tassan, CNRS, University of Rennes) and the pCMV-flag6c (Sigma) plasmids for mammalian expression. For the two hybrid screen, the prey clones were obtained by homologous recombination using cDNAs from the embryonic library described below and the pGADT7Rec vector (Clontech). The partial ZFPIP (ZFPIPp) cDNA was cloned into the pCMVflag6c vector (Sigma) for mammalian expression and into the pGEX-4T-1 vector (Amersham) for bacterial expression using, respectively, the *Eco*RI–*Bam*HI and the *Eco*RI–*Xho*I sites. The N-terminal and the C-terminal regions (respectively, N-ZFPIP and C-ZFPIP) of ZFPIP encoding cDNAs were cloned into *Bam*HI sites of the pCMVflag6c vector (Sigma). The ZFPIPp cDNA was also sub-cloned into the *Bam*HI and *Eco*RI sites of the pSPT18 and pSPT19 vectors (Roche). The HOXA9 cDNA was sub-cloned from pGEX-3X-HOXA9 (Dintilhac et al., 2005) to the *Eco*RI–*Bam*HI sites of the pGBKT7 and pCMVflag6c vectors. An *Eco*RI–*Sma*I fragment of CBP cDNA was extracted from pGEX-CBP (Dintilhac et al., 2005) and sub-cloned into *Eco*RI–*Xho*I blunt ended pGADGH to obtain pGADGH-CBP. The Pspf-PBX1A vector was kindly provided by C. Largman (University of California), and the pCMVflagTB3 by S. Hoshino (University of Tokyo).

4.2. cDNA library construction and yeast two hybrid screen

Total RNA was extracted from murine female developing genital tracts of E16.5–E18.5 embryos using the RNAgent Total Isolation System (Promega) and mRNAs were then purified with PolyATtract

mRNA Isolation System (Promega). The cDNAs were generated using random primers and SMART cDNA technology following MATCHMAKER Library Construction protocol (Clontech). The yeast two hybrid screen was performed with the MATCHMAKER Two-Hybrid System 3 (Clontech). The bait plasmid pGBKT7-PBX1B was co-transfected with the pGADT7Rec plasmid and the cDNA library into AH109 yeast strain in which homologous recombination could operate. Colony selection was performed using *HIS3*, *ADE2*, *lacZ* and *MEL1* selection and reporter genes. Prey plasmids from positive clones were isolated and were retransformed in yeast to check for reporter self-activation. Prey plasmids were sequenced with specific pGADT7 primers and identified by Blast analysis.

4.3. GST pull-down assay

Glutathione–Sepharose beads (Amersham Pharmacia Biotech) were loaded with 1 μg of bacterially expressed GST, GST-PBX1B, GST-HOX9 or GST-ZFPIPp. The pGBKT7-HOXA9, pGBKT7-PBX1B, pspf-PBX1A and pGADT7-ZFPIPp or other prey plasmids were used to perform a coupled in vitro transcription-translation in rabbit reticulocyte lysate containing ^{35}S-methionine and ^{35}S-cysteine as suggested by the manufacturer (TNT Quick Coupled Trancription/Translation System, Promega). Binding reaction of radiolabelled proteins and GST proteins was performed in a binding buffer BB1 (20 mM Hepes; 0.2 mM EDTA; 50 mM NaCl; 0.5 mM DTT; 2.5 mM $MgCl_2$; 0.1% NP40; 2% glycerol) at 4 °C overnight. After several washes with BB1 buffer, beads were boiled in protein-loading buffer, and eluted proteins were separated by SDS–PAGE. Polyacrylamide gels were then dried and analysed in a STORM 640 system using the ImageQuanT software (Molecular Dynamics).

4.4. Co-immunoprecipitation assay

Cos-7 cells were seeded (1×10^6 per dish) in 100 mm Petri dishes at 37 °C in 5% CO_2 in DMEM supplemented with 10% fetal calf serum (FCS) and grown overnight. They were then transfected by the calcium phosphate procedure using 5 μg of pcDNA3-HA-PBX1B and 5 μg of pCMVflag6c-HOXA9 or pCMVflag6c-ZFPIPp or pCMVflag6c-TB3. Transfected cells were lysed in TBS buffer (Tris 50 mM; NaCl 150 mM) 48 h following transfection. After a short sonication, the lysates were subjected to centrifugation and supernatants were incubated on agarose anti-flag M2 beads (Sigma) for 4 h at 4 °C. The pellets beads were then washed three times in TBS buffer (room temperature) and proteins were eluted with a 0.1 M glycine solution (pH 3.5). The elution products were then analyzed by SDS–PAGE and Western blotting using monoclonal anti HA (α-HA, Roche) and anti FLAG (α-FLAG, Sigma) antibodies.

4.5. Reverse transcription (RT) PCR and Quantitative RT real-time PCR

RNAs were purified with the Nucleospin kit (Macherey-Nagel) from adult tissues (liver, brain, kidney, muscle, female and male genital tracts) and from embryos (E9.5, E10.5, E12.5, E15.5 and E18.5). Purified and quantified RNA were analyzed on agarose gel. One microgram of total RNA from each time point was reverse transcribed to cDNA using random primer hexamers (New England Biolabs). PCR conditions were 94 °C for 45 s, annealing for 45 s at 50 °C during 30 cycles. PCR reactions were completed by a final extension at 72 °C for 10 min. As a control for total RNA integrity, Hypoxanthine Guanine Phosphoribosyl Transferase (HPRT) gene was used. The resulting products were analyzed on an ethidium bromide-stained 2% agarose gel.

For quantitative real-time reverse transcriptase PCR, primers were designed with Primer Express™ software (Applied Biosystems). Samples along with primers and Syber Green Master Mix (Applied Biosystems) were run in an ABI Prism 7000 SDS (Applied Biosystems) according to the manufacturer's protocol. Relative quantification of ZFPIP mRNA in each sample was calculated by comparison of their Ct values previously normalized with Ct values obtained for HPRT amplification. Experiments were run at least three times from different RNA extractions. The standard deviations reflect variability within triplicates. All the primer sequences used in RT PCR experiments are indicated in Table 1.

4.6. Immunocytochemistry

Cos-7 cells were seeded onto microscope cover slips in a 12-well plate and grown for 24 h to 60–70% confluence in DMEM supplemented with 10% FCS in 5% CO_2 at 37 °C. Using the TransFast™ transfection Reagent (Promega), Cos-7 cells were transfected with 1μg of plasmid DNA encoding for ZFPIPp-FLAG protein and grown for another 24 h as described above. Transfected cells were then fixed with PBS-Formaldehyde 3.7% (v/v) for 30 min at room temperature and submitted to immunocytochemistry as previously described (Roghi et al., 1998) using as primary antibody either FLAG M2 monoclonal antibody (α–FLAG, Sigma) or anti ZFPIP antibodies (α-ZFPIP). ZFPIP antibodies were generated in rabbits against two peptides (CENTDFGDSGRLYY and CLSPVKKRTRIDEIAS) according to the "double XP immunisation program" (Eurogentec). The immune sera obtained thus contained two types of antibody each recognizing 1

Table 1
Primers used in RT-PCR and EMSA experiments

	oligo – forward (5′–3′)	oligo – reverse (5′–3′)
RT-PCR		
ZFPIP-1	GCATTCTTACAGCCAACTGATG	TTGTATGTGCAAAACTGGCAAG
ZFPIP-2	GTACGTCGGATTGGGATACTGT	GACTTCGTTGTCATCCTCTTCC
ZFPIP-3	CTGTGATAGCAAATTGCAAAGC	TTCCACGCAGAATTTACACTTG
PBX1A/PBX1B	GAGTTAGCCAAGAAGTGCGG	CTGATAACATGGCGAAGGGT
HOXA9	AACAAACCAGATCGTGGAGC	GATGATACACTGCAGCAGGC
HPRT	CCTGCTGGATTACATTAAAGCACTG	GTCAAGGGCATATCCAACAACAAAC
Q RT-PCR		
ZFPIP	TTCTATAAAGGATGAGTTTGTGATTGC	TCCTGGACTGTGGCCATAGTAAC
PBX1B	CCAAAACGGCTGTCACAGC	AACATGGCGAAGGGTATCCA
HPRT	CCTGGTGAAAAGGACCTCTCG	GTCAAGGGCATATCCAACAACAAAC
EMSA	CTGCGATGATTTACGACCGC	GCGGTCGTAAATCATCGCAG

domain of the protein (Fig. 2A). Cells were then incubated with fluorescein conjugated goat anti-mouse IgG (FITC-IgGg, Jackson) or fluorescein conjugated goat anti-rabbit IgG (FITC-IgGg, Jackson). Controls were performed using either antibodies depleted by absorption with an excess of recombinant GST or GST-ZFPIPp or by omitting primary antibodies (immunocytochemistry performed with anti-FLAG antibody). Immunofluorescence was observed using a LEICA DM-RXA fluorescence microscope and images were collected with a charge-coupled device camera.

4.7. Protein extracts and western blot analysis

Adult mouse tissues (kidney, liver and thymus), whole mouse embryos (E12.5) and specific parts of E12.5 embryos (head, limb bud, tail) were dissected to obtain protein extracts. Female embryonic genital tracts and livers were obtained from bovine embryos, frozen and stored at −80°C. One gram of each tissue was washed several times in 0.9% NaCl and homogenized in lysis buffer (20 mM Hepes, pH 7.9; 1.5 mM $MgCl_2$; 0.2 mM EDTA; 1 mM DTT; 0.2% NP-40; 25% glycerol) containing a mix of proteases inhibitors (Sigma). Mechanical lysis was performed at 4 °C using a Polytron PT1600E (Bioblock). Extracts were filtered and NaCl was added to adjust concentration to 0.4 M. Extracts were kept 30 min at 4 °C, centrifuged 30 min (2000*g*, 4 °C) and supernatants were recovered. Transfected cells were lysed in TBS buffer at room temperature (Tris 50 mM; NaCl 150 mM). After a short sonication, the lysates were subjected to centrifugation and supernatants were kept for further analysis. Proteins (100 μg) were separated on SDS–polyacrylamide gel and electro-transferred onto PVDF membrane (Immobilon). Western blots were performed using α-FLAG, α-ZFPIP, depleted α-ZFPIP, β-tubulin and PCNA antibodies (Sigma).

4.8. Whole mount and in situ hybridization

Sense and anti-sense RNA probes were synthesized from linearized plasmids (pSPT18-ZFPIPp and pSPT19-ZFPIPp) using digoxygenin-labelled dUTP (Dig RNA Labelling Kit, Boehringer Manheim). Whole embryos were fixed overnight in 4% PFA–PBS at 4 °C and dehydrated in a graded methanol serie prior to storage at −20 °C. Whole-mount and hybridization was performed as described previously (Belo et al., 1997). Briefly, embryos were rehydrated in a graded methanol serie and treated with 5 μg/ml proteinase K (Qiagen). The embryos were re-fixed with 0.2% glutaraldehyde 4% PFA and washed in PBT (0.1% Tween 20-PBS) prior to hybridization overnight at 60 °C. Embryos were washed twice in 2× SSC-0.1% CHAPS at 65 °C, followed by two washes in maleic acid buffer and one in PBS. Embryos were then incubated with anti digoxigenin-AP Fab fragments (Roche). In situ RNA hybridization on paraffin sections was carried out as described (Dupe et al., 2003). Staining was visualized using BM purple substrate (Roche).

4.9. Electrophoretic mobility shift assay

EMSA were performed using complementary oligonucleotides containing consensus binding site for PBX1-HOX9 as described previously (Shen et al., 1997). Double-stranded ^{32}P end-labelled DNAs were incubated in a binding buffer (BB2: 10 mM Tris pH7.5, 75 mM NaCl, 1 mM DTT, 6% glycerol, 1 mM EDTA, and 2 μg of dIdC, 2 μg of BSA, 0.1 μg of salmon sperm DNA in a final reaction volume of 15 μl) with reticulocyte lysate reaction mixture containing HOXA9 or PBX1A or PBX1B or HOXA9/PBX1A or HOXA9/PBX1B proteins (TNT Quick Coupled Trancription/Translation System, Promega). After 10 min of incubation, bacterial lysate containing GST-ZFPIPp or GST were added to the binding reaction and experiments were continued for 20 min. Reaction mixtures were run on a 5% polyacrylamide gel in 0.5× Tris–Borate–EDTA buffer at 4 °C. Gels were dried and analysed in a STORM 640 system using the ImageQuaNT software (Molecular Dynamics).

Acknowledgments

I.P. wishes to thank sincerely people who provide us with vectors (Dr. C. Largman, Dr. M. Cleary, Dr. J.P. Tassan and Dr. S. Hoshino). We are grateful to Stéphanie Dutertre from the microscopy platform of IFR 140. We are also indebted to Dr. G. Salbert for helpful comments on the manuscript. A.L. was supported by a grant from the ''Conseil Régional de Bretagne''. This work was supported by the CNRS and by grants from ''Rennes Métropole'' and the ''Conseil Régional de Bretagne''.

References

Asahara, H., Dutta, S., Kao, H.Y., Evans, R.M., Montminy, M., 1999. Pbx-Hox heterodimers recruit coactivator–corepressor complexes in an isoform-specific manner. Mol. Cell Biol. 19, 8219–8225.

Bell, S.M., Schreiner, C.M., Waclaw, R.R., Campbell, K., Potter, S.S., Scott, W.J., 2003. Sp8 is crucial for limb outgrowth and neuropore closure. Proc. Natl. Acad. Sci. USA 100, 12195–12200.

Belo, J.A., Bouwmeester, T., Leyns, L., Kertesz, N., Gallo, M., Follettie, M., De Robertis, E.M., 1997. Cerberus-like is a secreted factor with neutralizing activity expressed in the anterior primitive endoderm of the mouse gastrula. Mech. Dev. 68, 45–57.

Berkes, C.A., Bergstrom, D.A., Penn, B.H., Seaver, K.J., Knoepfler, P.S., Tapscott, S.J., 2004. Pbx marks genes for activation by MyoD indicating a role for a homeodomain protein in establishing myogenic potential. Mol. Cell 14, 465–477.

Calvo, K.R., Knoepfler, P., McGrath, S., Kamps, M.P., 1999. An inhibitory switch derepressed by pbx, hox, and Meis/Prep1 partners regulates DNA-binding by pbx1 and E2a-pbx1 and is dispensable for myeloid immortalization by E2a-pbx1. Oncogene 18, 8033–8043.

Couly, G., Grapin-Botton, A., Coltey, P., Le Douarin, N.M., 1996. The regeneration of the cephalic neural crest, a problem revisited: the regenerating cells originate from the contralateral or from the anterior and posterior neural fold. Development 122, 3393–3407.

de Zulueta, P., Alexandre, E., Jacq, B., Kerridge, S., 1994. Homeotic complex and teashirt genes co-operate to establish trunk segmental identities in *Drosophila*. Development 120, 2287–2296.

Di Giacomo, G., Koss, M., Capellini, T.D., Brendolan, A., Popperl, H., Selleri, L., 2006. Spatio-temporal expression of Pbx3 during mouse organogenesis. Gene Expr. Patterns.

Dintilhac, A., Bihan, R., Guerrier, D., Deschamps, S., Bougerie, H., Watrin, T., Bonnec, G., Pellerin, I., 2005. PBX1 intracellular localization is independent of MEIS1 in epithelial cells of the developing female genital tract. Int. J. Dev. Biol. 49, 851–858.

Dupe, V., Matt, N., Garnier, J.M., Chambon, P., Mark, M., Ghyselinck, N.B., 2003. A newborn lethal defect due to inactivation of retinaldehyde dehydrogenase type 3 is prevented by maternal retinoic acid treatment. Proc. Natl. Acad. Sci. USA 24, 14036–14041.

Goudet, G., Delhalle, S., Biemar, F., Martial, J.A., Peers, B., 1999. Functional and cooperative interactions between the homeodomain PDX1, Pbx, and Prep1 factors on the somatostatin promoter. J. Biol. Chem. 274, 4067–4073.

Helmbacher, F., Pujades, C., Desmarquet, C., Frain, M., Rijli, F.M., Chambon, P., Charnay, P., 1998. Hoxa1 and Krox-20 synergize to control the development of rhombomere 3. Development 125, 4739–4748.

Hunt, P., Gulisano, M., Cook, M., Sham, M.H., Faiella, A., Wilkinson, D., Boncinelli, E., Krumlauf, R., 1991. A distinct Hox code for the branchial region of the vertebrate head. Nature 353, 861–864.

Kamps, M.P., Murre, C., Sun, X.H., Baltimore, D., 1990. A new homeobox gene contributes the DNA binding domain of the t(1;19) translocation protein in pre-B ALL. Cell 60, 547–555.

Kawakami, Y., Esteban, C.R., Matsui, T., Rodriguez-Leon, J., Kato, S., Belmonte, J.C., 2004. Sp8 and Sp9, two closely related buttonhead-like transcription factors, regulate Fgf8 expression and limb outgrowth in vertebrate embryos. Development 131, 4763–4774.

LaRonde-LeBlanc, N.A., Wolberger, C., 2003. Structure of HoxA9 and Pbx1 bound to DNA: Hox hexapeptide and DNA recognition anterior to posterior. Genes Dev. 17, 2060–2072.

Lee, M.S., Gippert, G.P., Soman, K.V., Case, D.A., Wright, P.E., 1989. Three-dimensional solution structure of a single zinc finger DNA-binding domain. Science 245, 635–637.

Mahaffey, J.W., 2005. Assisting Hox proteins in controlling body form: are there new lessons from flies (and mammals)? Curr. Opin. Genet. Dev. 15, 422–429.

Mahaffey, J.W., Griswold, C.M., Cao, Q.M., 2001. The *Drosophila* genes disconnected and disco-related are redundant with respect to larval head development and accumulation of mRNAs from deformed target genes. Genetics 157, 225–236.

Manley, N.R., Selleri, L., Brendolan, A., Gordon, J., Cleary, M.L., 2004. Abnormalities of caudal pharyngeal pouch development in Pbx1 knockout mice mimic loss of Hox3 paralogs. Dev. Biol. 276, 301–312.

Mann, R.S., Affolter, M., 1998. Hox proteins meet more partners. Curr. Opin. Genet Dev. 8, 423–429.

Moens, C.B., Selleri, L., 2006. Hox cofactors in vertebrate development. Dev. Biol. 291, 193–206.

Monica, K., Galili, N., Nourse, J., Saltman, D., Cleary, M.L., 1991. PBX2 and PBX3, new homeobox genes with extensive homology to the human proto-oncogene PBX1. Mol. Cell Biol. 11, 6149–6157.

Nourse, J., Mellentin, J.D., Galili, N., Wilkinson, J., Stanbridge, E., Smith, S.D., Cleary, M.L., 1990. Chromosomal translocation t(1;19) results in synthesis of a homeobox fusion mRNA that codes for a potential chimeric transcription factor. Cell 60, 535–545.

Popperl, H., Rikhof, H., Chang, H., Haffter, P., Kimmel, C.B., Moens, C.B., 2000. Lazarus is a novel pbx gene that globally mediates hox gene function in zebrafish. Mol. Cell 6, 255–267.

Redmond, L., Hockfield, S., Morabito, M.A., 1996. The divergent homeobox gene PBX1 is expressed in the postnatal subventricular zone and interneurons of the olfactory bulb. J. Neurosci. 16, 2972–2982.

Robertson, L.K., Bowling, D.B., Mahaffey, J.P., Imiolczyk, B., Mahaffey, J.W., 2004. An interactive network of zinc-finger proteins contributes to regionalization of the Drosophila embryo and establishes the domains of HOM-C protein function. Development 131, 2781–2789.

Roghi, C., Giet, R., Uzbekov, R., Morin, N., Chartrain, I., Le Guellec, R., Couturier, A., Doree, M., Philippe, M., Prigent, C., 1998. The Xenopus protein kinase pEg2 associates with the centrosome in a cell cycle-dependent manner, binds to the spindle microtubules and is involved in bipolar mitotic spindle assembly. J. Cell Sci. 111 (Pt 5), 557–572.

Sagerstrom, C.G., 2004. PbX marks the spot. Dev. Cell 6, 737–738.

Schnabel, C.A., Selleri, L., Jacobs, Y., Warnke, R., Cleary, M.L., 2001. Expression of Pbx1b during mammalian organogenesis. Mech. Dev. 100, 131–135.

Schnabel, C.A., Selleri, L., Cleary, M.L., 2003. Pbx1 is essential for adrenal development and urogenital differentiation. Genesis 37, 123–130.

Schock, F., Reischl, J., Wimmer, E., Taubert, H., Purnell, B.A., Jackle, H., 2000. Phenotypic suppression of empty spiracles is prevented by buttonhead. Nature 405, 351–354.

Selleri, L., Depew, M.J., Jacobs, Y., Chanda, S.K., Tsang, K.Y., Cheah, K.S., Rubenstein, J.L., O'Gorman, S., Cleary, M.L., 2001. Requirement for Pbx1 in skeletal patterning and programming chondrocyte proliferation and differentiation. Development 128, 3543–3557.

Shanmugam, K., Green, N.C., Rambaldi, I., Saragovi, H.U., Featherstone, M.S., 1999. PBX and MEIS as non-DNA-binding partners in trimeric complexes with HOX proteins. Mol. Cell Biol. 19, 7577–7588.

Shen, W.F., Montgomery, J.C., Rozenfeld, S., Moskow, J.J., Lawrence, H.J., Buchberg, A.M., Largman, C., 1997a. AbdB-like Hox proteins stabilize DNA binding by the Meis1 homeodomain proteins. Mol. Cell Biol. 17, 6448–6458.

Shen, W.F., Rozenfeld, S., Lawrence, H.J., Largman, C., 1997b. The Abd-B-like Hox homeodomain proteins can be subdivided by the ability to form complexes with Pbx1a on a novel DNA target. J. Biol. Chem. 272, 8198–8206.

Shen, W.F., Rozenfeld, S., Kwong, A., Kom ves, L.G., Lawrence, H.J., Largman, C., 1999. HOXA9 forms triple complexes with PBX2 and MEIS1 in myeloid cells. Mol. Cell Biol. 19, 3051–3061.

Taylor, H.S., 2000. The role of HOX genes in the development and function of the female reproductive tract. Semin. Reprod. Med. 18, 81–89.

Toresson, H., Parmar, M., Campbell, K., 2000. Expression of Meis and Pbx genes and their protein products in the developing telencephalon: implications for regional differentiation. Mech. Dev. 94, 183–187.

Wagner, K., Mincheva, A., Korn, B., Lichter, P., Popperl, H., 2001. Pbx4, a new Pbx family member on mouse chromosome 8, is expressed during spermatogenesis. Mech. Dev. 103, 127–131.

Waskiewicz, A.J., Rikhof, H.A., Hernandez, R.E., Moens, C.B., 2001. Zebrafish Meis functions to stabilize Pbx proteins and regulate hindbrain patterning. Development 128, 4139–4151.

Wimmer, E.A., Jackle, H., Pfeifle, C., Cohen, S.M., 1993. A Drosophila homologue of human Sp1 is a head-specific segmentation gene. Nature 366, 690–694.